LES AND ENTRAINMENT PARAMETRIZATION

M.K. MacVean
U.K. Meteorological Office
Bracknell, England

BACKGROUND

For the dry convective boundary layer, dimensional arguments suggest that the entrainment velocity w_e non-dimensionalized by the convective velocity scale w_* should be a function of the Richardson Number only. In practice, the expression

$$w_e/w_* = a_2/Ri_{w_*}$$

where

$$Ri_{w_*} = \frac{gh}{\theta_{v0}}\frac{\Delta\theta_v}{w_*^2}$$

appears appropriate, with $a_2 \sim 0.2$–0.25 (Driedonks,1982; Deardorff,1983). Here h is the boundary layer depth and $\Delta\theta_v$the jump in virtual potential temperature θ_v across the top of the boundary layer, while θ_{v0} is a constant reference value of θ_v. The convective velocity scale is given in terms of the surface buoyancy flux by

$$w_* = \left[\frac{gh}{\theta_{v0}}\left(\overline{w'\theta_v'}\right)_s\right]^{1/3} \tag{1}$$

Entrainment in the dry convective boundary layer is relatively easy to parametrize and there is some concensus on the validity of the formulae, because there are essentially only two non-dimensional parameters. However, when one considers the cloudy boundary layer, a range of additional physical effects come into play: namely, evaporation, radiative effects due to liquid water (most notably, cloud-top cooling) and microphysics. More importantly, perhaps, instead of considering a turbulent energy source remote from the interface at which the entrainment is occurring, as is the case for a dry convective boundary layer, the additional physical effects in the cloudy case represent sources of turbulent kinetic energy which may be located very close to the interface. In the circumstances it is not surprising that there is no general agreement about even the appropriate form of the functional dependence of the entrainment velocity in the cloudy boundary layer. Even if some concensus were to develop on the functional form, the determination of any constants would be rendered very difficult by the formidable difficulties in making appropriate and representative atmospheric measurements.

Nicholls and Turton (1986) suggested that evaporative effects could be taken into account by including dependence on the additional non-dimensional parameter $\Delta_m/\Delta\theta_v$, where $\Delta_m = 2\int_0^1 \delta\theta_v d\epsilon$. In this integral, $\delta\theta_v$ is the change in virtual potential temperature of cloudy air when a fraction ϵ of unsaturated air from above the inversion is mixed with it. They also used a generalized definition of the convective velocity scale (Deardorff, 1980) which may be written

$$w_* = \left[2.5\frac{g}{\theta_{v0}}\int_0^h \overline{w'\theta_v'}dz\right]^{1/3} \tag{2}$$

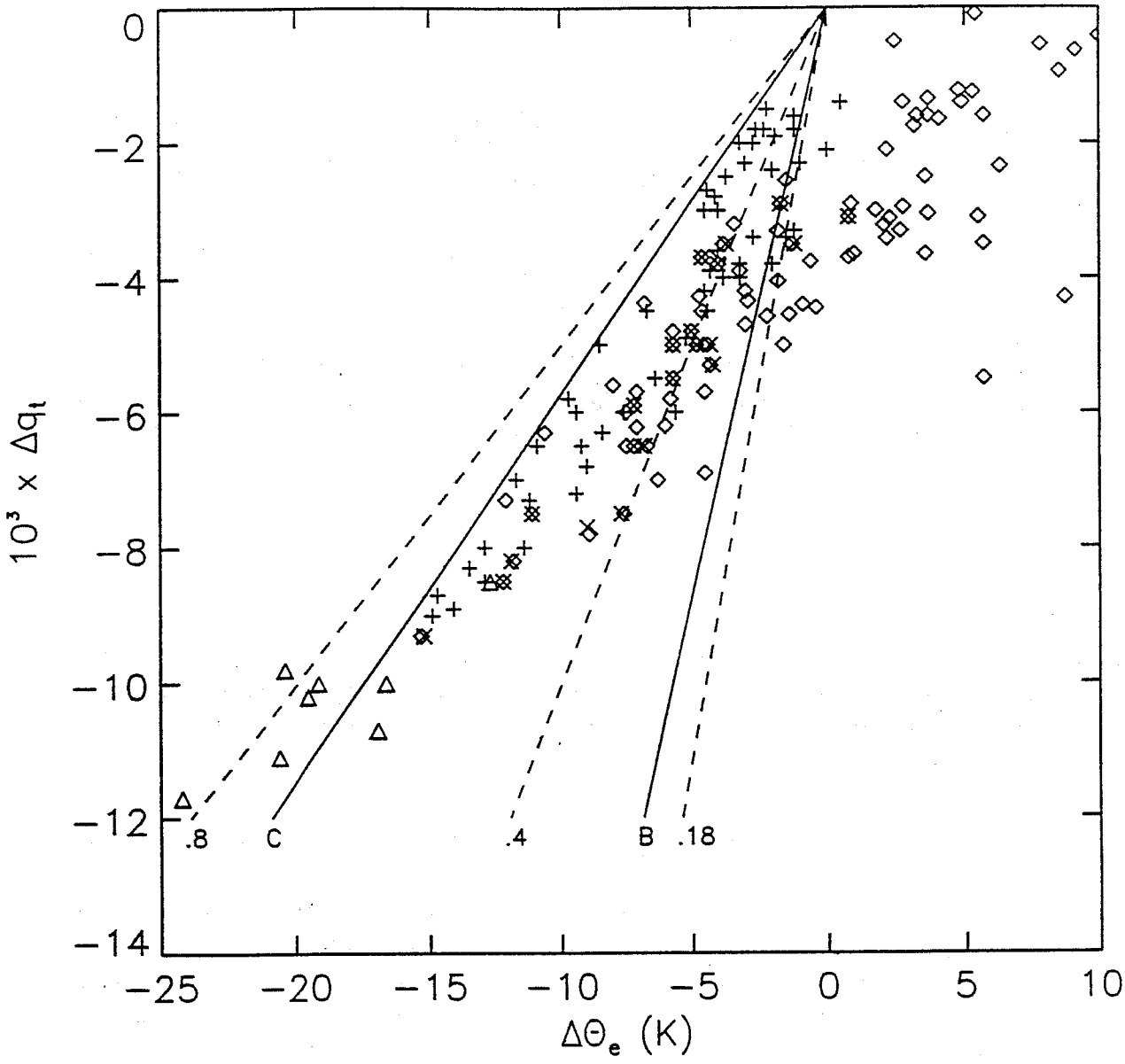

Figure 1: Cloud-top jumps in θ_e and q_t from observations. Stratocumulus data from Weaver and Pearson's Tables 3 and 4 are denoted by + and ×, respectively. Data on persistent stratocumulus and on trade cumulus from Kuo and Schubert's paper are denoted by ◇ and △, respectively. Also shown are the stability criteria of Randall and Deardorff (solid line B) and of MacVean and Mason (solid line C). The dashed lines are labelled by the constant values of R which they represent, which are those chosen for the initial conditions for the 3-D simulations presented later.

The data considered by Nicholls and Turton were obtained for $Ri_{w_*} \sim 250$ and $w_* \sim 0.6ms^{-1}$, yielding entrainment rates of 0.2–0.7 cms^{-1}. That is, the ratio w_e/w_* was 4–13 times that of a dry convective boundary layer at the same Richardson Number. The data showed the expected sense of dependence on $\Delta_m/\Delta\theta_v$, but it could provide no information about the dependence on the Richardson Number. It should be remembered that the entrainment rates presented by Nicholls and Turton were not direct measurements, but were derived from a one-dimensional model simulation of observed data It should also be noted that Duynkerke (1993) has recently suggested that a different parameter Δ_a,

where $\Delta_a = \int_0^1 \delta\theta_v/\epsilon d\epsilon$, is more relevant than Δ_m for quantifying the effects of evaporative cooling.

In view of the daunting difficulties in obtaining good data on entrainment rates from cloudy boundary layers, over a large range of conditions, the alternative of using data from large-eddy simulations to attempt to determine the functional form of the dependence of the entrainment rate appears attractive. It must be remembered, however, that LES data does not necessarily accurately represent reality and that for any conclusions from such data to be credible, those conclusions will have to be verified against as much good quality data from the atmospheric boundary layer as possible.

Until recently, much of the interest on entrainment in the cloudy boundary layer has focussed on cloud-top entrainment instability (CTEI). This instability is postulated to result from a positive feedback between turbulent mixing of saturated and unsaturated air and the evaporative cooling which may result. It has been suggested that this process might be responsible for the rapid breakup of stratocumulus sheets. The original criterion for this instability, proposed by Randall (1980) and Deardorff (1980), can be expressed in terms of the jumps in equivalent potential temperature and total water mixing ratio across cloud top. It takes the form $R > k_w$ where $R = c_p\Delta\theta_e/L\Delta q_t$ and k_w is a function of state, with a typical value of 0.23. This is, in fact, the condition for mixing of saturated and unsaturated air to result in a saturated parcel with density greater than that of either of the original components. Kuo and Schubert (1988) assembled observational data from various stratocumulus and trade-wind cumulus experiments and plotted $\Delta\theta_e$ against Δq_t, as in Fig.1. On this diagram we have also plotted stratocumulus observations reported by Weaver and Pearson (1990). The data clearly show more observations of persistent stratocumulus on the unstable side of Randall and Deardorff's CTEI criterion than on the stable side, calling the validity of the criterion into question. An alternative criterion was proposed by MacVean and Mason (1990), who considered the conditions under which there would be a net conversion from potential to kinetic energy as a result of mixing between saturated and unsaturated air in a two-layer system spanning cloud top. Their criterion can be expressed as $R > k_m$ where k_m is a function of state having a typical value of 0.7. It can be seen from Fig.1 that this criterion is at least consistent with most of the observational data. Other authors, including Siems *et. al.* (1990) and Duynkerke (1993), have also proposed alternative criteria. These are more similar to that of MacVean and Mason than to that of Randall and Deardorff. However, MacVean and Mason's stability boundary delimits the region in which persistent stratocumulus is observed, rather more closely than those proposed by other authors.

MacVean (1993) reported the results of a series of integrations with a two-dimensional large-eddy model, which provide further support for this criterion. The integrations were carried out at $5m$ resolution and with surface fluxes and radiative effects excluded, leaving evaporative cooling as the only source of turbulent kinetic energy. Figure 2 shows how the decay rate of the total cloud water content varies with R and with the subgrid model used. Irrespective of the sub-grid model, a very marked increase in the decay rate is observed at around the theoretical critical value of R. In this region of parameter space, entrainment due to evaporative cooling is sufficient, on its own, to dissipate an initially uniform cloud deck within a period of about one hour, suggesting that cloud-top entrainment instability may indeed be a potent mechanism for the rapid breakup of stratocumulus.

THREE-DIMENSIONAL LES SIMULATIONS

The study by MacVean (1993) did not concentrate on entrainment rates or velocities as such. What is ultimately required are values of entrainment velocity over a large range of

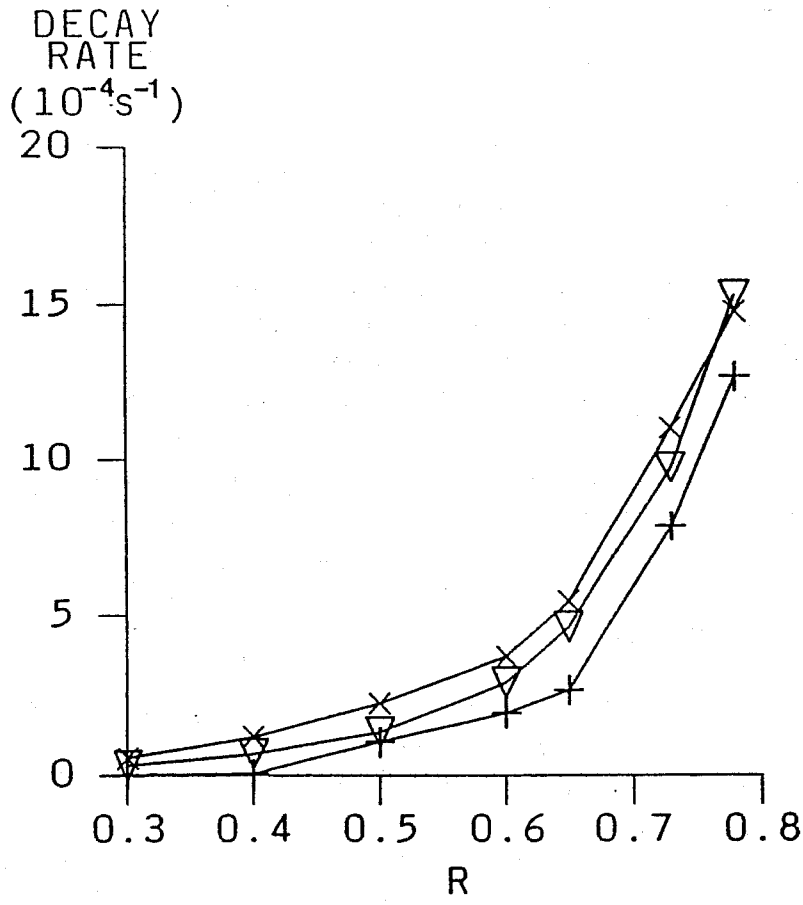

Figure 2: Variation with R of the e-folding decay rate for the domain-integrated liquid water content from integrations using various subgrid models. For more details, see MacVean and Mason (1990).

parameter space, and for these values to be credible, they really need to be obtained from three-dimensional simulations. Such a programme is underway, but only a very limited sample of preliminary results are currently available. In the integrations reported here, we have used a resolution of $20m$ in the vertical and $40m$ in the horizontal. Furthermore, we have limited the horizontal extent of the domain to $2.5km \times 2.5km$. An investigation of the effect of coarsening the resolution in two-dimensional integrations has shown that results are not significantly effected until the resolution is poorer than about 50m. Nevertheless, we eventually plan to carry out 3-D simulations at higher resolution than currently used, for a limited number of points in parameter space, as resources permit. For the present, we prefer to use the available resources to enable a wider exploration of parameter space, at relatively low resolution. We have already seen signs in some of the 3-D simulations that the limited horizontal domain size may be having an undesirable effect. These qualifications should be borne in mind when considering the results, but hopefully their effect is quantitative rather than qualitative.

The integrations were carried out with a non-hydrostatic, Boussinesq, finite difference model using T_l (the liquid water static energy divided by c_p) and q_t (the total water mixing ratio) as conserved variables. The domain was periodic in the horizontal and extended to $2.5km$ in the vertical. The upper $1km$ was configured as a damping layer, to absorb any upward propagating gravity waves. The initial conditions (Fig.3) were loosely

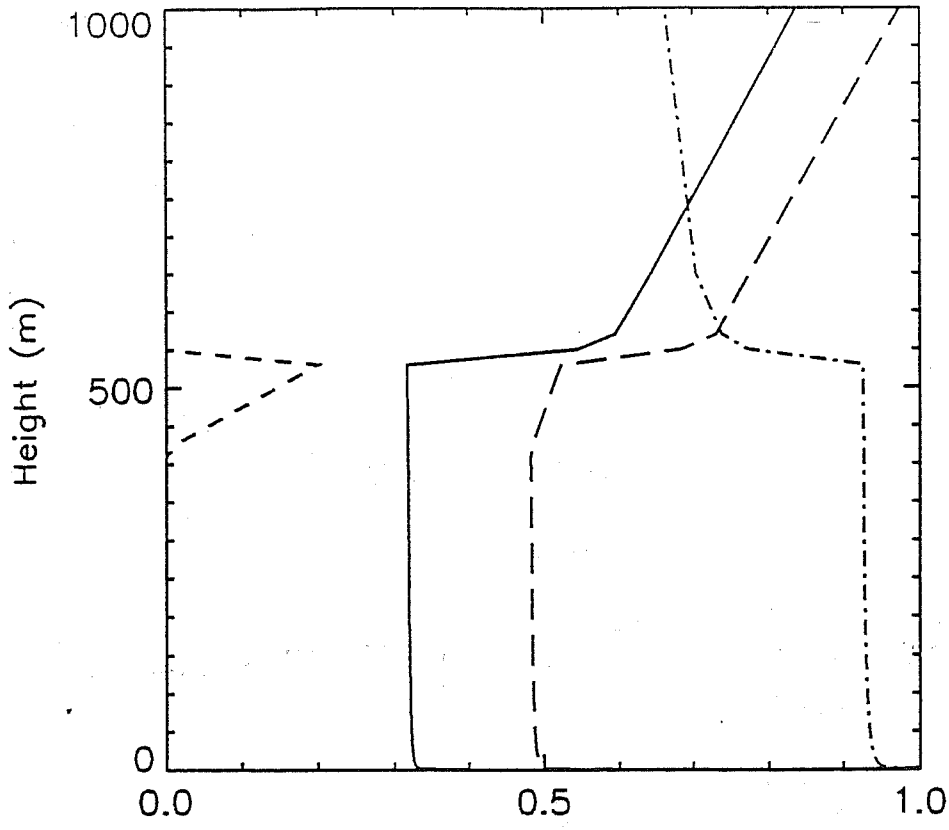

Figure 3: Vertical profiles illustrating the initial conditions for the integration with $R = 0.4$. The solid line is T_ℓ, the dash-dotted line q_t, the short-dashed line q_ℓ and the long-dashed line θ_v. The horizontal axis runs from $286K$ to $296K$ for T_ℓ and θ_v, from 0 to 10^{-3} for q_ℓ and from 0 to 10^{-2} for q_t. Only the lower $1km$ of the domain is shown.

based on observations from the KONTUR experiment (Hoeber, 1982). The geostrophic wind was set to $7ms^{-1}$ and surface heat fluxes of $6.5Wm^{-2}$ (sensible) and $37.5Wm^{-2}$ (latent) were imposed. A very simple parametrization of cloud-top radiative cooling was included, with a transmission function given by $\exp(-144q_\ell)$, where q_ℓ is the liquid water mixing ratio. The radiative heat flux at the top of the cloud was fixed at $30Wm^{-2}$. The initial conditions shown were for $R = 0.4$; those for other values of R were obtained by varying the T_ℓ and q_t profiles above the boundary layer, while maintaining the illustrated θ_v profile. In order to provide a good measure of entrainment, a passive tracer variable was carried, which was initialized to zero within the boundary layer and unity above. The most satisfactory measure of entrainment velocity appears to be the time rate of change of Q_{999}, the volume integral, per unit horizontal area, of this variable over all points for which its value is less than 0.999. Unfortunately, this measure was not calculated for all of the integrations discussed here. Other measures available were the time rate of change of the inversion height ($ZINVA$ or $ZINVB$), as determined from the local Richardson Number profile or the height of occurrence of the minimum in the turbulent vertical flux of T_ℓ, respectively, or the volume integral, per unit horizontal area, of the passive tracer up to the inversion height. The latter is denoted as Q_{ZINVA} or Q_{ZINVB}, according to which definition of inversion height is used. All these alternative measures do not share with Q_{999} the advantage of being non-decreasing.

The first set of results to be discussed (run 470) are for an initial state with $R = 0.18$,

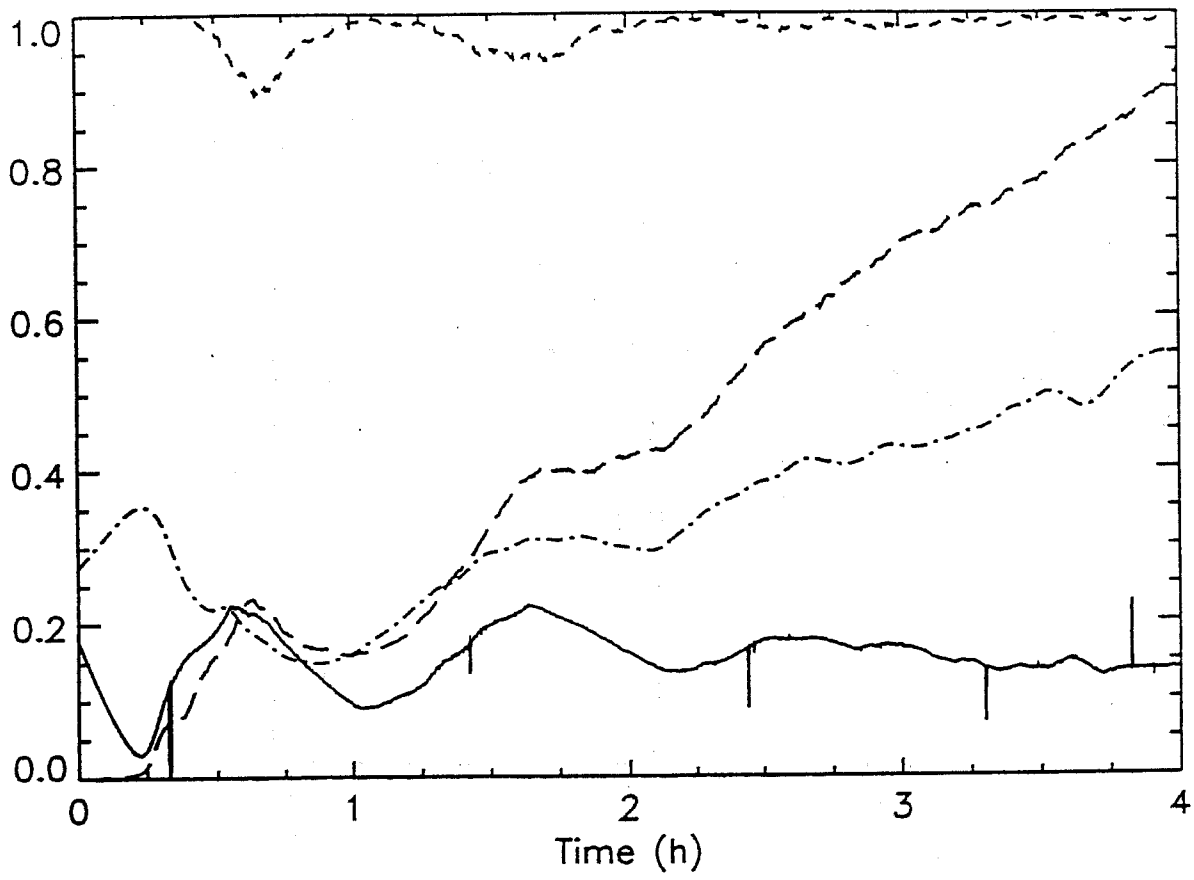

Figure 4: Timeseries of various quantities from the integration with $R = 0.18$ initially. The solid line is R_{AV}, the dash-dotted line q_l^{TOT}, the long-dashed line Q_{ZINVA} and the short-dashed line the cloud fraction $CLFRAC$. Q_{ZINVA} has been normalized by the value $200m$ and q_l^{TOT} by 3×10^5

at which point in parameter space we would not expect evaporative cooling to be an active source of turbulence, since R is smaller than the critical value derived by Randall and by Deardorff. The time development of various gross properties over the $4h$ period of the integration is presented in Fig.4. The value of R averaged over all grid columns containing cloud (R_{AV}) is seen to oscillate between about 0.025 and 0.225 over the first $2h$ of integration, but becomes relatively constant at a value close to 0.15 thereafter. The scatter in values of R on individual grid columns is substantial, with typical maximum values of about 0.6 and even a very small number of points with $R > k_m = 0.7$. Thus there is , in fact, some generation of turbulent energy through evaporative cooling but the major source is the cloud-top radiative cooling. Because the integrations are initialized with a very small perturbation to an otherwise horizontally homogeneous state, the first 15min or so of the integration is dominated by radiative cooling of the horizontal mean state near cloud top. This cooling leads to the initial increase in the total cloud water content (q_l^{TOT}) seen in Fig.4. It also generates a mean state which is statically unstable, the resulting convection leading, over the following 30min, to a sharp reduction in the total cloud water content and a reduction in cloud cover to a minimum of about 90%. After about $2h$, these transients have decayed and the integration settles down to a statistically quasi-steady state, with a cloud cover greater than 95% and a total cloud water content which is increasing linearly, as a result of the surface moisture flux and the net cooling of

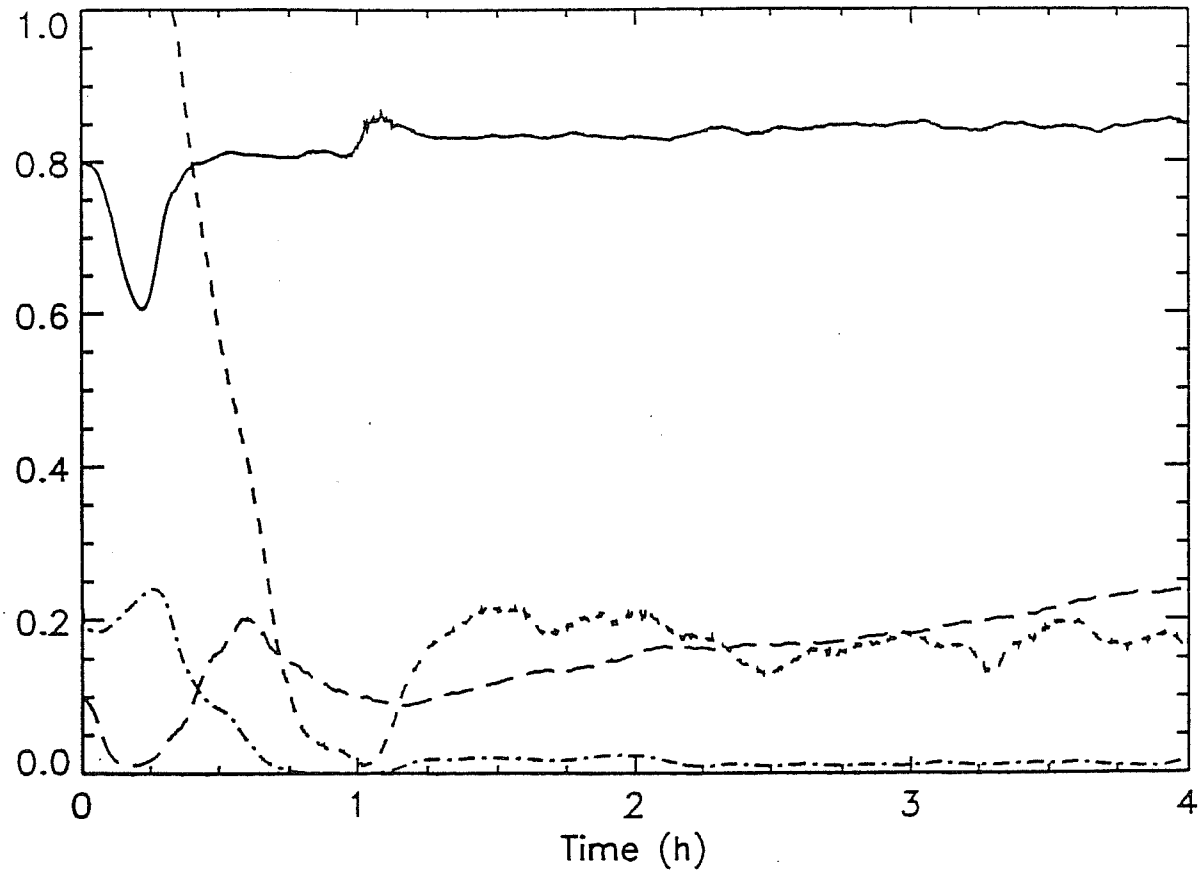

Figure 5: As Fig.4, but for the integration with $R = 0.8$ initially

the boundary layer. The entrainment measure shown for this integration is Q_{ZINVA}; over the last $2h$ of the integration it yields an entrainment velocity of $1.4cms^{-1}$.

The second integration to be presented (run 471) started from initial conditions with $R = 0.8$ which, according to MacVean and Mason's criterion, should exhibit CTEI. The time development is displayed in Fig.5. During the first 15min, the combination of radiative and strong evaporative cooling leads to the generation of very strong convective motions and during the following 30 min the cloud cover and total cloud water content are reduced almost to zero. Over this latter period the entrainment velocity, estimated from Q_{ZINVA}, is about $3.6cms^{-1}$. The cloud cover does not, however, remain close to zero. Over the second hour of integration, it is around 20%, the cloud taking the form of cumulus convection organized into a line by the mean wind. The entrainment velocity at this time is typically $0.4cms^{-1}$. For the last $2h$ of the integration the typical cloud cover is somewhat lower, at around 15%, with an entrainment velocity of about $0.2cms^{-1}$. During this integration a very large range of entrainment velocities was seen, while the average value of R was relatively constant. The calculated entrainment velocities declined monotonically with the cloud cover, probably reflecting the averaging of a changing proportion of cloudy points with a high local entrainment rate and unsaturated points where we would expect entrainment to be much slower. In this integration, the convective cloud observed over the final $2h$ was maintained against dissipation through rapid entrainment at cloud top, by the surface flux of moisture. This was clearly demonstrated by extending the integration beyond $4h$ but with the surface fluxes turned off, when all the cloud was observed to evaporate within $1h$.

The third integration to be discussed (run 472) lies between the two extremes already

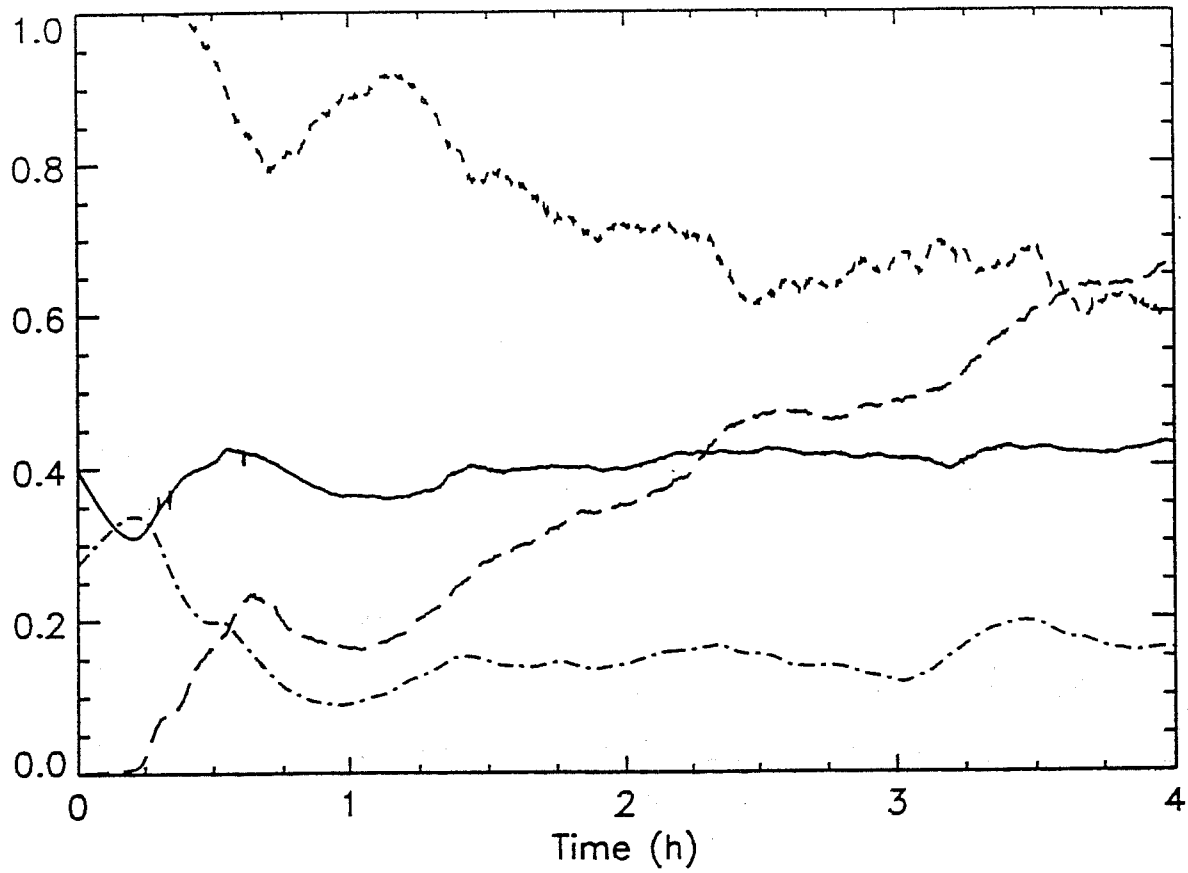

Figure 6: As Fig.4, but for the integration with $R = 0.4$ initially

considered, with $R = 0.4$ initially. The time development is summarized in Fig.6. Again, the first hour or so of the integration was dominated by strong transient adjustments to the radiative and evaporative cooling near cloud top. After that, the average value of R remained quite close to its original values, with less than 3% of individual grid columns having $R > 0.7$. There was very little overall trend in the total liquid water content over the last $3h$, although there was a slow overall decline in the cloud fraction. It is not clear from the length of record we have, whether this decline is a continuing long-term trend or whether the 60–70% cloud cover observed over the last $2h$ is close to some quasi-equilibrium value. The entrainment velocity measured by fitting a straight line to the Q_{999} timeseries over the final $3h$ of the simulation is about $0.9cms^{-1}$. A similar value can be obtained from the Q_{ZINVA} timeseries, although the fit is not as good in that case. The decrease in the entrainment velocity relative to that calculated in run 470, even though the value of R is greater in the present case, is again presumably attributable to the decrease in the cloudiness.

DISCUSSION

Table 1 summarizes the results from these integrations, together with those from a pair of runs (465 and 466), not discussed above, in which the sensitivity to the magnitude of the radiative flux at cloud top was investigated. In interpreting the data presented, and in comparing it with that presented by Nicholls and Turton, the uncertainties in determining representative values of parameters must always be borne in mind.

Increasing the radiative flux to $68Wm^{-2}$ in run 465 resulted in substantial increases in w_e, w_* and w_e/w_*, relative to their values in run 466. However, it appears that this may

TABLE 1

Summary of various properties of the integrations discussed. In general, the values given are averages over the last $2h$ of the integration. However, three sets of values are given for 471, representing averages over the periods 900–1800s, 3600–7200s and 8100–14400s, labelled by subscripts 1, 2 and 3 respectively. Ranges are given for the cloud fraction ($CLFRAC$) where variations were large. In 465, the variation of R_{AV} about the time mean value shown was much larger (0.3–0.42) than in the other integrations. The w_* values given were calculated from (2), using $\theta_{v0} = 288.65K$. In calculating Ri_{w_*}, $\Delta\theta_v$was taken as $2.5K$.

Run	R_{AV}	$CLFRAC$	h (m)	$w_* (ms^{-1})$	Ri_{w_*}	$w_e (cms^{-1})$	$w_e/w_* (\times 100)$
470	0.15	0.95	640	0.54	173	1.3	2.32
465	0.35	0.60–0.85	630	0.65	127	1.5	2.31
472	0.40	0.65	625	0.52	196	0.9	1.73
466	0.55	0.35–0.50	580	0.49	205	0.7	1.43
471_1	0.81	1.00 ↓ 0.05	540	1.01	45	3.6	3.56
471_2	0.83	0.20	565	0.51	185	0.4	0.78
471_3	0.84	0.15	575	0.50	195	0.2	0.40

not have been a direct effect, as increasing the radiative flux lead to a rather different time variation in R and to an increased cloud fraction. With hindsight, it would have been better to have checked the sensitivity of the entrainment velocity to radiative cooling in a situation where the cloud cover was expected to remain complete. Similar difficulties are apparent with interpretation of the results for varying R. It had originally been anticipated that the entrainment velocity would show a general increase with R, that increase being most steep near the critical value of 0.7. While it is true that the largest entrainment rate observed was for the initial state with the highest R, this was only sustained for a very limited time, during the period in which the original cloud deck was dissipated. If we consider the quasi-equilibrium behaviour observed in the last $2h$ of the integrations, we observe the opposite of what had originally been anticipated: namely, a decrease in the entrainment velocity as R is increased. The explanation of this appears to be related to the decrease in the cloud cover observed with increasing R. Our measure of the entrainment rate is a bulk one, representing some sort of weighted average of the local entrainment velocities both in unsaturated grid columns and in those containing cloud. While it seems likely that the entrainment velocity in grid columns containing cloud is a strongly increasing function of R, this increasing entrainment velocity results in an equilibrium cloud cover which decreases so strongly that the contribution to our bulk measures of entrainment from the columns containing cloud, actually decreases.

The values of Ri_{w_*} tabulated for all the cases except 465 and 471_1, lie within a relatively narrow range from 173 to 205, yet the values of w_e/w_* vary by a factor of more than 5, indicating the important role of factors other than the Richardson Number. Although we have not calculated them here, we would expect Δ_m and Δ_a to increase with R. Since $\Delta\theta_v$ is approximately constant, our data would, therefore, seem to show an inverse dependence of entrainment velocity on $\Delta_m/\Delta\theta_v$ or $\Delta_a/\Delta\theta_v$, contrary to the finding of Nicholls and Turton. The resolution of this apparent conflict presumably again lies in the variation of the cloud fraction, which would have to be included in any parametrization. Comparing the data from run 470, which had almost complete cloud cover, with the average of Nicholls and Turton's stratocumulus cases 511, 526, 528 and 620, we note that w_e/w_* is 0.0232 in the former and only 0.0077 in the latter. The Richardson Number in run 470 is

only 173, compared with 286 in Nicholls and Turton's data. We would therefore expect w_e/w_* to be larger in run 470, although the difference is considerably greater than would be predicted by the simple inverse dependence on Ri_{w_*} which holds in the dry convective case.

It is interesting to note that, except for cases 465 and 471_1, the values of w_* calculated from (2) are within about 10% of those calculated from (1), on the basis of the surface buoyancy flux and boundary layer height alone. One might have expected the turbulent kinetic energy production due to evaporative and radiative cooling to have been more substantially reflected in w_* in all the cases considered here. It seems that only in the cases with the largest cloud-top flux (run 465) or largest evaporative cooling (run 471_1) was there a significant effect on w_*. The effect was transient in run 471, because of the decay in the cloud fraction.

One must be very wary of suggesting parametrizations for larger-scale models from such a limited set of results. In spite of this, it is tempting to conclude by provisionally suggesting that cloud fraction might be usefully parametrized as a function of R decreasing from 1 at $R < 0.23$ to zero at some value of R greater than 0.7. There is some limited observational support for this in papers by Betts and Boers (1990) and Weaver and Pearson (1990). Betts and Boers characterized four regimes, which they labelled "stratocumulus" (99% cloud cover), "broken" (73%), "cumulus" (12%) and "clear" (0%). Corresponding values of R, calculated from the data they give, are 0.34,0.53,0.69 and 0.72. These values are at least in qualitative agreement with the results of our simulations. The experimental data presented by Weaver and Pearson (1990) showed an underlying trend for flights with frequent sightings of holes and splits in the cloud deck to sample the highest values of R, while flights with solid cloud sampled the lowest values, which is again qualitatively consistent with the suggestion for a parametrization made above. The currently available evidence does not, however, allow any conclusions to be drawn even as to a definitive set of parameters on which the entrainment velocity will depend, much less the functional form of the dependence. Clearly it is going to be a great challenge to devise an appropriate series of integrations from which to determine this with any certainty. Even if this challenge is successfully met, the difficulties in implementation in a GCM or NWP model may not be insignificant. The additional problems are likely to stem from the relatively poor resolution of such models, particularly in the vertical. For example, values of R calculated with a grid spacing of several hundred metres may be very different to those calculated with a resolution of order $10m$. This is, of course, not a new problem, affecting many existing parametrizations, for example those depending on Richardson Number.

REFERENCES

Betts, A.K. and R. Boers, 1990: A cloudiness transition in a marine boundary layer. *J. Atmos. Sci.*, **47**, 1480–1497.

Deardorff, J.W., 1980: Cloud-top entrainment instability. *J. Atmos. Sci.*, **37**, 131–147.

Deardorff, J.W., 1983: A multi-limit mixed layer entrainment formulation. *J. Phys. Oceanog.*,**13**,988–1002.

Driedonks, A.G.M., 1982: Models and observations of the growth of the atmospheric boundary layer. *Bound. Layer Meteor.*, **23**, 283–306.

Duynkerke, P.G., 1993: The stability of cloud top with regard to entrainment: amendment of the theory of cloud-top entrainment instability. *J. Atmos. Sci.*, **50**, 495–502.

Hoeber, H., 1982: KONTUR: Convection and Turbulence Experiment—Field Phase Report. *Hamburger Geophysikalische Einzelschriften*, Reihe B, No.1.

Kuo, H., and W.H. Schubert, 1988: Stability of cloud-topped boundary layers. *Quart. J. Roy. Meteor. Soc.*, 114, 887–916.

MacVean, M.K., 1993: A numerical investigation of the criterion for cloud-top entrainment instability. *J. Atmos. Sci.*, **50**, 2481–2495.

MacVean, M.K., and P.J. Mason, 1990: Cloud-top entrainment instability through small-scale mixing and its parametrization in numerical models. *J. Atmos. Sci.*, **47**, 1012–1030.

Nicholls, S. and J.D. Turton, 1986: An observational study of the structure of stratiform cloud sheets: Part II. Entrainment. *Quart. J. Roy. Meteor. Soc.*, **112**, 461–480.

Randall, D.A., 1980: Conditional instability of the first kind upside-down. *J. Atmos. Sci.*, **37**, 125–130.

Siems, S.T., C.S. Bretherton, M.B. Baker, S. Shy and R.T. Breidenthal, 1990: Buoyancy reversal and cloud-top entrainment instability. *Quart. J. Roy. Meteor. Soc.*, **116**, 705–739.

Weaver, C.J. and R. Pearson Jr, 1990: Entrainment instability and vertical motion as causes of stratocumulus breakup. *Quart. J. Roy. Meteor. Soc.*, **116**, 1359–1388.